



ISSN: 0975-833X

Available online at <http://www.journalcra.com>

INTERNATIONAL JOURNAL
OF CURRENT RESEARCH

International Journal of Current Research
Vol.3, Issue, 5, pp.078-083, May, 2011

RESEARCH ARTICLE

VIBRATIONAL SPECTROSCOPIC STUDY AND NBO ANALYSIS ON TRANEXAMIC ACID USING DFT METHOD

Muthu, S^{1*} and Prabhakaran, A²

¹Department of Physics, Sri Venkateswara College of Engineering, Sriperumbudur-602 105, India

²Departments of Physics, Pallavan College of Engineering, Kanchipuram-631 502, India

ARTICLE INFO

Article History:

Received 11th January, 2011
Received in revised form
18th February, 2011
Accepted 15th March, 2011
Published online 14th May 2011

Key Words:

FT-IR, FT-Raman, NBO analysis,
HOMO, LUMO and DFT

ABSTRACT

In this work, we report a combined experimental and theoretical study on molecular structure, Vibrational spectra and NBO analysis of tranexamic acid (TA). The FT-Raman and FT-IR spectra of TA were recorded in the solid phase. The molecular geometry, harmonic vibrational frequencies and bonding features of TA in the ground state have been calculated by using density functional method (B3LYP) with standard 6-31G (d,p) basis set. Stability of the molecule arising from hyper conjugative interactions, charge delocalization has been analyzed using natural bond orbital (NBO) analysis. The calculated HOMO and LUMO energies show that charge transfer occurs within the molecule. The theoretical FT-IR and FT-Raman spectra for the title molecule have been constructed.

© Copy Right, IJCR, 2011 Academic Journals. All rights reserved

INTRODUCTION

Tranexamic acid (TA) is chemically 4-(aminomethyl) cyclohexane-1-carboxylic acid is a synthetic derivative of the amino acid lysine that exerts its antifibrinolytic effect through the reversible blockade of the lysine binding sites on plasminogen molecules (Thoresen *et al.*, 1981). TA is useful in a wide range of haemorrhagic conditions. The drug reduces postoperative blood losses and transfusion requirements in a number types of surgery (Brown *et al.*, 1997 and Ido *et al.*, 2004), with potential cost and tolerability advantages over aprotinin, and appears to reduce rates of mortality and urgent surgery in patients with upper gastrointestinal haemorrhage. TA reduces menstrual blood loss and is a possible alternative to surgery in menorrhagia and has been used successfully to control bleeding in pregnancy. In the present study, FT-IR, FT-Raman spectral investigation of TA has been performed using density functional theory (DFT). The redistribution of electron density (ED) in various bonding and antibonding orbital and E(2) energies have been calculated by natural bond orbital (NBO) analysis by DFT method to give clear evidence of stabilization originating from the hyper conjugation of various intra-molecular interactions. The HOMO and LUMO analysis have been used to elucidate information regarding charge transfer within the molecule.

MATERIALS AND METHODS

The compound TA was purchased from sigma-Aldrich chemical company (USA) with a stated purity of greater than 97% and it was used as such without further purification. The FT-Raman spectrum of TA has been recorded using 1064 nm

line of Nd-YAG laser as excitation wavelength in the region 100-4000 cm^{-1} on Bruker Model IFS 66 spectrophotometer. The FT-IR spectrum of this compound was recorded in the region 400-4000 cm^{-1} on IFS 66V Spectrophotometer using KBr pellet technique with a scanning speed of 30 $\text{cm}^{-1} \text{min}^{-1}$ and the spectral resolution of 4.0 cm^{-1} . The observed experimental and calculated FT-IR and FT-Raman spectra are shown in Figs. 1 and 2. The spectral measurements were carried out at Sophisticated Analytical Instrumentation Facility (SAIF), IIT, and Chennai.

Computational details

The entire calculations was performed at Density functional theory (DFT) levels with a Pentium Intel (R) core 2 quad 2.40 GHz personal computer using Gaussian 03W (Frisch *et al.*, 2004) program package, invoking gradient geometry optimization (Schlegel, 1982). The optimized structural parameters were used in the vibrational frequencies calculations at the DFT/B3LYP/6-31G (d,p) level to characterize all stationary points as minima. The natural bonding orbitals (NBO) calculation (Glendering *et al.*, 1998) were performed using NBO 3.1 program as implemented in Gaussian 03W (Frisch *et al.*, 2004) package at DFT/6-31G(d,p) level in order to understand various second-order interaction between the filled orbitals of one subsystem and vacant of another subsystem, which is measure of the intermolecular delocalization or hyper conjugation. The Raman activities (Si) calculated with Gaussian 03 were converted to relative Raman intensity using Raint program (Michalska, 2003) by the expression:

*Corresponding author: muthu@svce.ac.in

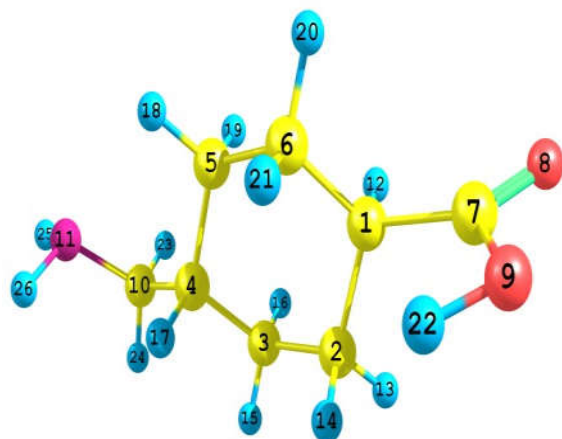


Fig.1. The atom numbering for TA molecule

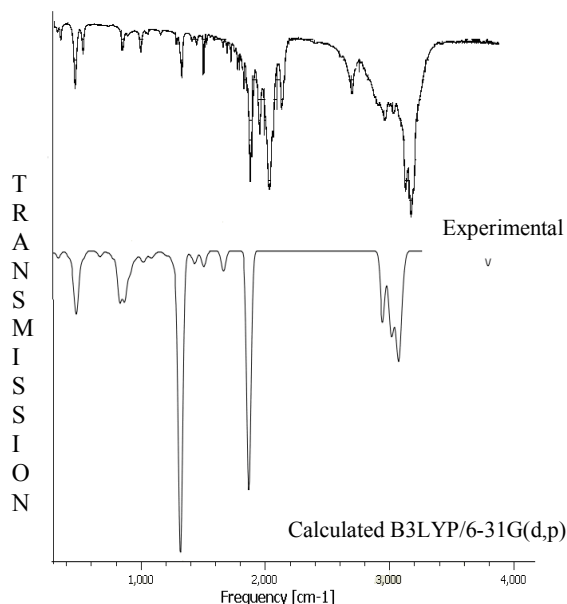


Fig. 2. FTIR spectra of TA calculated and experimental

$$I_i = 10^{-12} (v_0 - v_i)^4 (1/v_i) S_i$$

Where I_i is the relative Raman intensity, S_i the Raman activities, v_i is the wave number of normal modes and v_0 denotes the wave number of the excitation laser (Michalska, 2005).

RESULTS AND DISCUSSION

Molecular geometry

The labeling of atoms in TA is given in Fig 3. The optimized geometrical parameters (bond length and bond angles) by DFT/B3LYP with 6-31G (d,p) basis set are listed in Table 1, a general priority for reproducing the experimental bond length

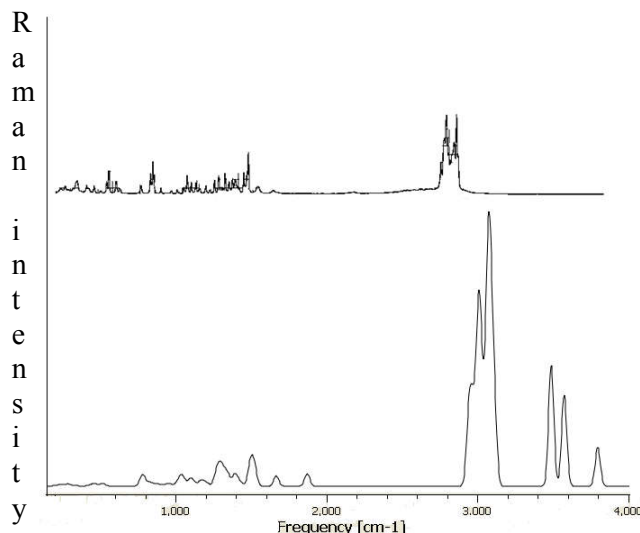


Fig. 3. FT-Raman spectra of TA calculated and experimental

taken from the Ref (Carl kemnitz, 2002) is not present among DFT/B3LYP levels. However, all the bond and bond angles computed with the DFT/B3LYP level shows excellent agreement with available experimental results.

Vibrational assignments

Vibrational spectral assignments have been performed on the recorded FT-IR and FT-Raman spectra based on the theoretically predicted wave numbers by density functional method (B3LYP) using 6-31G (d,p) basis set and have been collected in Table 2. Comparison of the frequencies calculated at B3LYP method with experimental values reveals the overestimation of the calculated vibrational modes due to neglect of anharmonicity in real system. In our study we have followed scaling factor for B3LYP/6-31G (d,p); 0.9608 (Scoott *et al.*, 1996).

C-H Vibration

The hetero aromatic structure shows the presence of C-H stretching vibration in the region 3100-3000 cm^{-1} which is the characteristic region for the ready identification of C-H stretching vibration (Varsanyi, 1973). In this region, the bands are not affected appreciably by the nature of substituents. The vibration assigned by chemcraft program package at 2971 to 2952 cm^{-1} by B3LYP/6-31G (d,p) levels, show good agreement with weak FT-Raman band at 2952 cm^{-1} wear assigned to the C-H stretching vibration in the aromatic ring. In general in-plane and out-of-plane aromatic C-H deformations occur in the region 1300-1000 cm^{-1} and 600-1000 cm^{-1} respectively. The C-H in-plane bending vibration computed at 1057, 1196 and 1277 cm^{-1} by B3LYP/6-31G(d,p) method shows good agreement with experimental values. The C-H out of plane bending vibration band appears in FT-IR at 845 cm^{-1} and in FT-Raman at 852 cm^{-1} shows good agreement with computed DFT (B3LYP) method at 838 cm^{-1} . In general C-H vibration computed by both methods shows good agreement with experimental observation as well as literature data.

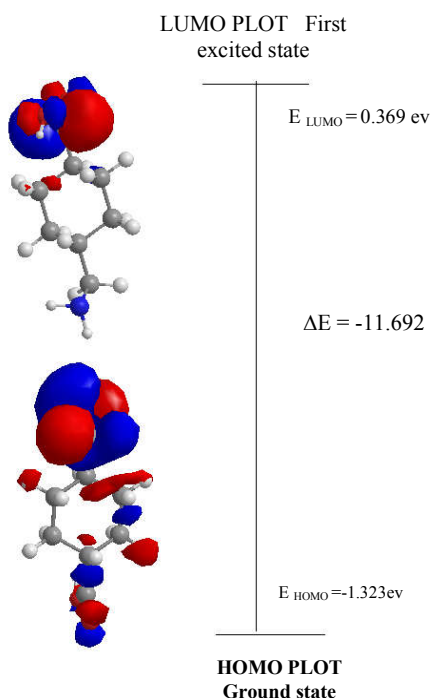


Fig. 4. The atomic orbital HOMO – LUMO composition of the frontier molecular orbital for TA

Table 1. Comparison between the calculated DFT and experimental values of geometrical parameters for TA

Bond length	B3LYP/6-31G(d,p)	experimental	Bond angle	B3LYP/6-31G(d,p)	experimental
C1-C2	1.545	1.523	C1-C7-O9	116.2	119.9
C1-C6	1.545	1.523	C3-C2-H13	110.4	109.4
C1-C7	1.526	1.509	C3-C2-H14	108.9	109.5
C1-H12	1.095	1.113	C2-C3-C4	112.2	109.4
C2-C3	1.536	1.523	C2-C3-H15	109.6	109.4
C2-H13	1.096	1.113	C2-C3-H16	109	109.4
C2-H14	1.1	1.113	H13-C2-H14	106.3	105.3
C3-C4	1.538	1.523	C4-C3-H15	110.3	109.4
C3-H15	1.097	1.113	C4-C3-H16	109.1	109.5
C3-H16	1.1	1.113	C3-C4-C5	110.5	109.5
C4-C5	1.538	1.523	C3-C4-C10	111.4	109.5
C4-C10	1.535	1.523	C3-C4-H17	107.5	109.5
C4-H17	1.104	1.113	H15-C3-H16	106.4	105.3
C5-C6	1.534	1.523	C5-C4-C10	112.1	109.4
C5-H18	1.093	1.113	C5-C4-H17	107.8	109.5
C5-H19	1.1	1.113	C4-C5-C6	112.1	109.5
C6-H20	1.096	1.1129	C4-5-H18	109.6	109.5
C6-H21	1.101	1.113	C4-C5-H19	108.8	109.5
C7-O8	1.206	1.208	C10-C4-H17	107.4	109.5
C7-O9	1.365	1.338	C4-C10-N11	111.3	109.5
O9-H22	0.968	0.9719	C4-C10-H23	108.8	109.4
C10-N11	1.467	1.4379	C4-C10-H24	108.7	109.5
C10-H23	1.098	1.113	C6-C5-H18	110.8	109.5
C10-H24	1.105	1.113	C6-C5-H19	109	109.5
N11-H25	1.017	1.02	C5-C6-H20	110.5	109.5
N11-H26	1.018	1.02	C5-C6-H21	108.9	109.5
			H18-C5-H19	106.4	105.3
			H20-C6-H21	106.3	105.3
Bond angle	B3LYP/6-31G(d,p)	experimental			
C2-C1-C6	110.5	109.5	O8-C7-O9	119.6	119.9
C2-C1-C7	112.1	109.4	C7-O9-H22	110.1	109.5
C2-C1-H12	108.4	109.5	N11-C10-H23	107.7	109.4
C1-C2-C3	111.3	109.5	N11-C10-H24	113.8	109.4
C1-C2-H13	109.9	109.4	C10-N11-H25	110.1	109.4
C1-C2-H14	109.8	109.5	C10-N11-H26	109.7	109.4
C6-C1-C7	112.7	109.5	H23-C10-H24	106.3	105.3
C6-C1-H12	108.4	109.5	H25-N11-H26	106.1	109.4
C1-C6-C5	111.2	109.5			
C1-C6-H20	109.9	109.5			
C1-C6-H21	109.9	109.5			
C7-C1-H12	104.6	109.5			
C1-C7-O8	124.3	119.9			

O-H vibrations

The O-H group gives rise to three vibration (stretching, in-plane bending and out-of-plane bending vibration). The O-H group vibrations are likely to be most sensitive to the

environment, so they show pronounced shifts in the spectra of the hydrogen bonded species. The hydroxyl stretching vibrations are generally (Sajan *et al.*, 2006) observed in the region around 3500 cm^{-1} . In the case of the un-substituted phenols it has been shown that the frequency of O-H stretching vibration in the gas phase is 3657 cm^{-1} (Michalska *et al.*, 1996). Similarly in our case a strong FT-IR band at 3423 cm^{-1} is assigned to O-H stretching vibration. The hydrogen bonding effect through hydroxyl group leads to dimmer conformation OH stretching mode calculated at 3652 cm^{-1} which is much closer to the FT-IR experimental observation at 3423 cm^{-1} .

The O-H in-plane bending vibration in the phenols, in general lies in the region $1150\text{--}1250\text{ cm}^{-1}$ and is not much affected due to hydrogen bonding unlike to stretching and out-of-plane bending frequencies. The medium band in FT-IR spectrum at 1162 and 1195 cm^{-1} is assigned O-H in-plane bending vibration. Theoretically computed value at 1143 and 1163 cm^{-1} by B3LYP method shows good agreement with recorded spectrum. The O-H out-of-plane bending mode for the free molecule lies below 300 cm^{-1} and it is beyond the infrared spectral range of the present investigation. However, for the associated molecule (Varsanyi, 1973) the O-H out-of-plane bending mode lies in the region $517\text{--}710\text{ cm}^{-1}$ in both intermolecular and intramolecular association, the frequency is at a high value than in free O-H. In our present investigation a strong band observed in FT-IR spectrum at 555 cm^{-1} is

assigned to O-H out-of-plan bending vibration, the theoretically computed value by B3LYP shows the same kind of vibration at 520 and 646 cm^{-1} are assigned to O-H out-of-plane bending vibration.

Table 2. Vibrational wavenumbers obtained for TA at B3LYP/6-31G(d,p) and compared with experimental value

Experimental Wave number		Calculated B3LYP/6-31G(d,p)			Vibrational Assignment
FT-IR	FT-Raman	Scaled	IR- Inten	Raman Activity	
		31	7	1	τ -Ring
		60	1	0	τ -Ring
		110	1	0	Breathing
	133	140	2	0	Breathing
	182	184	17	0	γ -C-COOH
		218	21	1	γ CCC
		225	0	0	γ CCC
	217	236	17	1	γ -C-NH ₂
	253	276	1	3	γ -C-NH ₂
	330	324	8	2	γ -C-NH ₂
	381	402	6	1	β OH
	420	434	3	1	γ CCC
	452	442	16	3	γ CCC
	472	475	467	71	γ CCC
	526		496	5	γ OH+ ρ CH ₂
	555	520	519	8	ρ -CH ₂
	668		645	7	γ OH
	702	701	711	2	β CC
	769		750	8	β CC
	788	767	772	2	β CC
		790	799	59	γ CH
	845	845	837	57	γ CH
			875	21	ν CC
			881	6	ν CH
	903		911	6	ν CC
	921	920	926	4	γ CH
		955	964	8	β CCC
			988	8	β CC
	1010	1008	1004	3	β CH
		1029	1032	2	β CH
			1045	6	β CH
	1059	1058	1056	1	β CH
			1070	2	β CH
	1120	1120	1119	1	β CH
			1141	1	β OH
	1162	1154	1161	4	β OH
	1195	1196	1195	6	β CH
	1227	1232	1221	14	β CH ₂
	1255	1254	1243	12	β CH ₂
			1263	6	β CH ₂
			1270	333	ν C-OH
	1280	1276	1275	32	β CH
	1289		1288	1	β CH
			1296	4	τ CH ₂
		1302	1302	2	τ CH
	1330	1325	1329	0	β OH
			1339	0	ν CC
			1344	2	ν CO
	1356	1351	1357	1	δ CH ₂
	1385	1374	1379	15	τ CH ₂
	1434		1436	0	β CH
			1441	4	β CH
		1445	1446	14	β CH
	1453		1455	0	τ CH ₂
	1538	1465	1463	2	δ NH ₂ + ν CC
	1635	1652	1642	25	ν C=O+ ν CC
			1799	294	ν C=O
		2842	2830	83	ν_s CH ₂
	2864	2868	2855	16	ν_s CH ₂
	2878	2880	2883	16	ν_s CH ₂
			2891	37	ν_s CH ₂
		2901	2902	9	ν_s CH ₂
			2907	53	ν_s CH ₂
	2921	2932	2932	35	ν_s CH ₂
			2949	52	ν CH
		2952	2952	5	ν CH
			2959	33	ν CH
			2967	43	ν CH
			2989	17	ν CH
			3352	1	ν_s NH
	3423		3435	0	ν_{as} NH
			3648	18	ν OH

ν - stretching; ν_s - symmetric stretching; ν_{as} - asymmetric stretching; β - in-plane bending; γ - out of plane bending; δ -scissoring; ρ -wagging; ρ - rocking; τ - twisting; τ - ring

Table 3. Second order perturbation theory analysis of Fork matrix in NBO basis for TA

Donor(i)	Type	ED/e	Acceptor(j)	Type	ED/e	E(2) (kcal/mol)
C4-C10	σ	1.96	C2-C3	σ^*	.015	2.16
			C3-C4	σ^*	.019	0.99
			C4-C5	σ^*	0.19	1.07
			C4-H17	σ^*	0.02	0.55
N11-H25	σ	1.98	N11-H25	σ^*	0.006	2.13
			C4-C10	σ^*	0.02	3.09
			C10-H23	σ^*	0.018	3.03
			LP(1)N11	σ^*	0.02	0.87
LP(1)O9	σ	1.96	C10-H23	σ^*	0.01	1.12
			C10-H24	σ^*	0.03	7.39
			C1-C7	σ^*	0.06	7.46
			C7-O8	σ^*	0.01	2.24
LP(2)O9	σ	1.82	C7-C8	σ^*	0.20	47.40
			C1-C7	σ^*	0.06	2.61
LP(1)O8	σ	1.97	C7-O9	σ^*	0.09	1.01
			C1-C7	σ^*	0.022	17.07
LP(2)O8	σ	1.855	C1-C7	σ^*	0.09	34.57
			C7-O9	σ^*	0.09	34.57

Table 4. HOMO LUMO energy calculated by B3LYP/6-31G(d,p) method

Method	B3LYP/6-31G(d,p)
HOMO	-11.323eV
LUMO	0.369eV
Energy gap (ΔE)	-11.692eV

C-C ring stretching

In benzonitriles, the distance between two carbon atoms changes the ring angles because of its substituents groups such as cyanogens. There are six equivalent C-C bonds in benzene and consequently there will be six C-C stretching vibrations. The bands are observed at 1538 and 1632 cm⁻¹ in FT-IR are identified as C-C stretching vibrations. The same vibration appear in the FT-Raman spectrum at 1652 cm⁻¹. The theoretically scaled C-C stretching vibrations by DFT method are at 1642⁻¹ shows excellent agreement with recorded FT-IR and FT-Raman spectral data. The ring in-plane vibrations have given rise to weak bands across the low frequency region, that is to say, below 1000cm⁻¹ the bands at 751 and 989 cm⁻¹ have been assigned to C-C in-plane bending vibrations.

CH₂ bending vibrations

In the present study, the band around 1280cm⁻¹ in FT-IR is assigned to CH₂ wagging mode which agrees with the result (1281cm⁻¹) of (Matulkova et al) in the case of 4-aminotriazole adipic acid (4atadip). The harmonic frequencies calculated by B3LYP/6-31G(d,p) method falling in the region 1340-1277 cm⁻¹, which are in agreement with the earlier report (Matulkova et al). The calculated frequencies 1297 and 1359 cm⁻¹ are assigned to twisting of CH₂. Matulkova et al. reported the CH₂ twisting frequency observed in the range 1223-1314 cm⁻¹ of 4atadip. In the present work CH₂ twisting vibration is assigned to medium Raman band at 1276 and 1302 cm⁻¹. However, the DFT value is in agreement with the experimental value. The band appeared around 1356 cm⁻¹ in FT-IR is assigned to CH₂ scissoring mode. The computed CH₂ rocking mode is appears at 520 cm⁻¹ in DFT. The FT-IR band at 526 cm⁻¹ and Raman band at 535 cm⁻¹ are assigned to CH₂ rocking mode, which agree favourably with Matulkova et al. and also find support from theoretical value. Billes et al. assigned CH-in-plane bending vibration appeared at 1419, 1114, 1411 and 1126 cm⁻¹, respectively in 1H-1,2,3-and 1D-1,2,3-triazoles. In view of above bands appeared at 1435 cm⁻¹

in FT-Raman and 1445 in FT-IR spectrum are assigned to C-H in plane bending mode. The calculated frequencies in the region 828-956 cm^{-1} for C-H out-of- plane bending fall in the FT-IR and FT-Raman values of 845-920 cm^{-1} .

NH₂ vibration

The molecule under investigation possesses only one NH₂ group and hence one expects one symmetric and one asymmetric N-H stretching vibration in NH₂ group. In all the primary aromatic amines, the N-H stretching frequency occurs in the region 3300-3500 cm^{-1} (Bellamy, 1980). Hence the weak bands in FT-IR spectrum wear located at 3320-3232 cm^{-1} assigned to N-H asymmetric and symmetric stretching vibration, respectively in NH₂ group. These assignments agree well with the earlier report (Bellamy, 1980). The scaled NH₂ asymmetric and symmetric stretching are in the range 3439-3356 cm^{-1} in B3LYP/6-31G(d,p). The computed NH₂ scissoring vibration at 1465 cm^{-1} in B3LYP/6-31G(d,p) is in agreement with the expected experimental value at 1465 cm^{-1} . The C-NH₂ out-of-plane and in-plane bending vibration at 253 and 381 cm^{-1} observed at FT-Raman spectrum agree well with theoretically obtained values using B3LYP/6-31G (d,p).

COOH vibration

Carboxylic acid dimer is formed by strong hydrogen bonding in the solid and liquid state vibrational analysis of carboxylic acid group is made on the basis of carbonyl group and hydroxyl group. The C=O stretch of carboxylic acid is identical to the C=O stretch in ketones, which is expected in the region 1740-1660 cm^{-1} (Vein *et al.*, 1991). The C=O bond formed by P_{π} - P_{π} between C and O intermolecular hydrogen bonding reduces the frequencies of the C=O stretching absorption to a greater degree than does intermolecular H bonding because of the different electro-negativities of C and O, the bonding are not equally distributed between the two atoms. The lone pair of electrons on oxygen also determines the nature of the carbonyl groups. In our present study a strong band observed in FT-IR spectrum 1635 cm^{-1} is assigned to C=O stretching vibrations, which show good agreement with B3LYP scaled value at 1642 cm^{-1} . Two other characteristic carboxylic group vibrations are C-O stretching and C-O bending vibrations. They are expected in the region 1140-395 cm^{-1} and 1700-875 cm^{-1} depending on whether monomeric, dimeric or other hydrogen bonded species are present. Generally the C-O stretching mode appears at lower frequencies than C-O bending vibration.

NBO Analysis

Natural bond orbital analysis gives the most accurate possible natural Lewis structure picture of \emptyset because all orbital are mathematically chosen to include the highest possible percentage of the electron density. Interaction between both filled and virtual orbital space information is correctly explain by the NBO analysis, it could enhance the analysis of intra and inter molecular interaction. The second order Fock matrix was carried out to evaluate donor (i)-acceptor (j) i.e. donor level bonds to acceptor level bond interaction in the NBO analysis (Szafran *et al.*, 2007). The result of interaction is a loss of occupancy from the concentration of electron NBO of the idealized Lewis structure into an empty non-Lewis orbital. For

each donor (i) and acceptor (j), the stabilization energy $E^{(2)}$ associates with the delocalization $i \rightarrow j$ is estimated as

$$E^{(2)} = \Delta E_{ij} = q_i (F(i,j))^2 / (\epsilon_j - \epsilon_i)$$

Where q_i is the donor orbital occupancy, ϵ_i - and ϵ_j are diagonal element and $F(i,j)$ is the off diagonal NBO Fock matrix element. Natural bond orbital analyses provide an efficient method for interaction among bond, and also provide a convenient basis for investigation charge transfer or conjugative interaction in molecular systems. Some electron donor orbital, acceptor orbital and the interaction stabilization energy resulted from the second order micro-disturbance theory are reported (James *et al.*, 2006 and Jun-na *et al.*, 2005). The larger $E^{(2)}$ value the more intensive is the interaction between electron donors and acceptor i.e. the more donation tendency from electron donors to electron acceptors and the greater the extent of conjugation of the whole system (Sebastian *et al.*, 2010). Delocalization of electron density between occupied Lewis-type (bond or lone pair) NBO orbitals and formally unoccupied (anti bond or rydberg) non Lewis NBO orbital correspond to a stabilizing donor-acceptor interaction. NBO analysis has been performed on the TA molecule at the DFT/B3LYP/6-31G(d,p) level in order to elucidate, the intra molecular rehybridization and delocalization of electron density within the molecule. The LP(2) O9 is seen to be lowest-occupancy and to be primarily delocalized into anti bond C₇-O₈. The $E^{(2)}$ values and types of transition as shown Table 3.

HOMO and LUMO analysis

Highest occupied molecular orbital (HOMO) and the lowest unoccupied molecular orbital (LUMO) and very important parameters for quantum chemistry. We can determine the way the molecule interacts with other species. Hence, they are called the frontier orbitals. HOMO, which can be thought the outermost orbital containing electrons, trends to give these electrons such as an electron donor. On the other hand; LUMO can be thought the innermost orbital containing free places to accept electrons (Gece *et al.*, 2008). The HOMO and LUMO energy calculated by B3LYP /6-31G(d,p) method are shown in Table 4. This electronic transition absorption corresponds to the transition from the ground to the first excited state and is mainly described by an electron excitation from the HOMO to the LUMO. The HOMO is located over the NH₂ group, the HOMO > LUMO transition implies an electron density transfer to ring and acid group. The atomic compositions of the frontier molecular orbital are shown in Fig. 4. The calculated self-consistent field (SCF) energy of TA is -519.11 A.U

Conclusion

The spectral studies such as FT-IR, FT-Raman for TA was carried out for the first time. A complete vibrational and molecular structure analysis has been performed based on the quantum mechanical approach by DFT (B3LYP) calculations. The assignments made at DFT level of theory with only reasonable deviations from the experimental values seem to be correct. The calculated absorption maxima values at DFT (B3LYP) level almost correlate with the experimental value. The theoretically constructed FT-IR, FT-Raman spectra

coincide with experimentally observed FT-IR, FT-Raman. NBO reflects the charge transfer within the molecule. HOMO and LUMO orbitals have been visualized.

REFERENCE

- Bellamy, L.J. 1980. The infrared spectra of complex molecule vol 2
- Billes, F, Endredi, H, and Keresztury, G, 2000. Vibrational spectroscopy of triazoles and tetrazole. *J. Mol. Struct., (Theochem)*. 530 : 183.
- Brown, R.S, Thwaites, B.K, Mongan, P.D, 1997. Tranexamic acid is effective in decreasing postoperative bleeding and transfusions in primary coronary artery bypass operations: a double-blind, randomized, placebo-controlled trial. *Anesth Analg, J Obstet Gynecol.*, 85: 963-70.
- Carl Kemnitz, 2002. Chemoffice ultra 10, Trial version.
- Frisch, M. J, *et al.*, 2004. Gaussian 03W, Revision C.02. Wallingford: Gaussian Inc.,
- Gece, G, 2008. The use of quantum chemical methods in corrosion inhibitor studies. *Corros. Sci.*, 50: 2981.
- Glendering, E.D, Read, A.E, Carpenter, J.E, and Weinhold, F, 1998. NBO Version 3.1. TCI, University of Wisconsin, Madison..
- Ido, K, Neo, M, Asada, Y *et al.*, 2000. Reduction of blood loss using tranexamic acid in total knee and hip arthroplasties. *Arch Orthop Trauma Surg.*, 120:518-20
- James, C, Amal Raj, A, Rehunathan, R, Hubert Joe, I, Jayakumar. V.S. 2006. *J. Raman Spectrosc*, 379 1381
- Jun-na, L, Zhi-rang, C, Shen-fang, Y and Zhejiag, J, 2005. *Univ. Sci.* 6B (2005) 584
- Matulkova, I, Nemeč, I, Teubner, K, Nemeč, P, and Micka, Z, 2008. Novel compound of 4-amino-1,2,4-triazole with dicarboxylic acids - crystal structures, vibrational spectra and non-linear optical properties. *J. Mol. Struct.*, 873 : 46.
- Michalska, D and Wysokinski, R, 2005. Chem. The prediction of Raman spectra of platinum(II) anticancer drugs by density functional theory, *Phys. Lett*, 403: 211.
- Michalska, D, 2003. Raint Program, Wroclaw University of Technology.
- Michalska, D, Bienko, D.C., Bienko, A.J.A , and Latajka, Z, 2008. Density Functional, Hartree-Fock and MP2 studies on the vibrational spectrum of phenol. *J. Phys Chem.*, 100: 1186.
- Sajan, D, Hubert Joe, I, Jayakumar, V.S, and Zaleshki, J, 2006. Structural and electronic contributions to hyperpolarizability in methyl p-hydroxy benzoate. *J. Mol. Struct.*, 785: 43
- Schlegel, H. B, 1982. Optimization of equilibrium geometries and transition structures. *J. Comput. Chem.*, 3: 214-218.
- Scott, A.P, Radom, L, 1996. Harmonic vibrational frequencies: an evaluation of Hartree-Fock, Møller-Plesset, quadratic configuration interaction, density functional theory, and semiempirical scale factors. *J. Phys. Chem.*, 100: 16502
- Sebastian, S, and Sundaraganesan, N, 2010. The spectroscopic (FT-IR, FT-IR gas phase, FT-Raman and UV) and NBO analysis of 4-Hydroxypiperidine by density functional method. *Spectrochim Acta*, A 75 : 941.
- Szafran, M, Komasa, A, and Adamska, E.B, 2007. Crystal and molecular structure of 4-carboxypiperidinium chloride (4-piperidinecarboxylic acid hydrochloride *J. Mol. Struct. (THEOCHEM)* 827: 101.
- Thorsen S, Clemmenson I, Sottrup-Jensen L *et al.* 1981. Adsorption to fibrin of native fragments of known primary structure from human plasminogen. *Biochim Biohys Acta.*, 668: 377-87.
- Varsanyi, G, 1973. Assignment of vibrational spectra of seven hundred Benzene derivatives, 1/2, Academic kiaclo, Budapest.
- Vein, D.L, Colthup, N.B, Fateley, W.G and Grasselli, J.G, 1991. The Handbook of Infrared and Raman Characteristic Frequencies of Organic Molecules, Academic press, San Diego.
